

Coexistence of extended and localized states in one-dimensional systems

A. M. C. Souza^{1,2,4}, R. F. S. Andrade^{3,4}

¹Departamento de Física, Universidade Federal de Sergipe 49.100-000, São Cristóvão - Brazil.

²Department of Physics, University of Central Florida, Orlando, FL 32816, USA.

³Instituto de Física, Universidade Federal da Bahia, 40210-340 Salvador Brazil.

⁴National Institute of Science and Technology for Complex Systems.

E-mail: randrade@ufba.br

Abstract. Mobility edge transitions from localized to extended states have been observed in two and three dimensional systems, for which sound theoretical explanations have also been derived. One-dimensional lattice models have failed to predict their emergence, offering no clues on how to actually probe this phenomenon in lower dimensions. This work reports results for a class of tight-binding models with electron-mass position dependence, for which localized-extended wave function transitions can be identified. We show that it is possible to control the density of localized and extended states by tuning the transition-related parameter for a continuous range of energy values. Mathematically exact results for extended or localized states are derived in two extreme conditions of this parameter, as well as an exact energy value for the mobility edge transition in the intermediate regime. Our framework provides a clear point of view on the phenomena and can also be harnessed for setting up experiments to probe to precisely evaluate the associated mobility edges using state-of-the-art technology.

1. Introduction

The localized-extended wave function transition in quantum systems has been one of the most active areas of study in the condensed matter physics during the last decades. As a matter of fact, accurate phase transition diagrams based on the energy of the quantum particle and a suitable control parameter explain most of the experimental findings. In general, models based on the one-electron tight-binding Hamiltonian are able to clearly identify the transition the two types of wave functions. Among the different systems, with one (or more) control parameters, that induce localized-extended transition one may quote those displaying random disorder [1], incommensurate potentials [3], quantum percolation [4, 5], correlated disorder [2], and the variation of clustering properties in complex networks [6, 7].

For systems that undergo mobility edge transitions, localized and extended states can coexist at different energies: for a fixed value of the control parameter, a critical energy level separates localized from extended states, allowing for a fine tuning of the systems conduction properties by simply altering the energy flux to the system. Such a property adds substantial versatility to devices and circuit components, what explains the large efforts made to tackle this yet unsolved problem. We remind that the precise experimental measurements of the mobility edge energy, which has been actively pursued, was until recently an elusive issue even for three dimensional systems[8]. Similar subtleties are also found in one-dimensional systems where, despite significant efforts, further details on the presence of localized-delocalized transition with mobility edges are still to be found on both theoretical and practical sides [9, 10]. Indeed, the first experimental evidences of such an effect in a one-dimensional quasi-periodic optical lattice have been reported only recently [11]. Those results are supported by a theoretical description of the system in the continuum limit[12]. Surprisingly, after performing performing the tight-binding approximation, it was found that the mobility edge disappears [12]. Indeed, we are lead to the well-studied Aubry-Andre model, with a usual extended/localized transition where all states are either localized or delocalized, depending only of the on the strength of the control parameter [3, 13].

This work intends to fill that gap by analyzing the properties of a well defined physical system on a regular lattice, where the transition between extended and localized wave functions is clearly gauged by one parameter associated with the effective electrons mass. In particular, we consider a one-dimensional tight binding model where the electron-mass is defined according to its position along the lattice and reproduce the usual two- and three-dimensional mobility-edge landscape, accounting for the presence of extended and localized states in distinct regions of the spectrum. One amazing aspect of the model is the fact that it allows for exact analytical results in the two limiting cases, where only extended or localized states are present. These results are in full agreement with the numerical integration of the systems equations which, as usual in such circumstance, are also used to explore the intermediary regime where states of both classes coexist.

The rest of this work is organized as follows: In Sec. II we present a brief review of the used formalism leading to position dependent masses, which is followed by the derivation of the equivalent tight-binding Hamiltonian in Sec. III. Sec. IV is details the exact analytical treatment to account for the limiting behavior of the model, where only extended or localized states exist. Results for the intermediate parameter value, where the two kinds of states coexist are discussed in Sec. V, while concluding remarks and possible applications of the formalism are brought in Sec. VI.

2. Position dependent mass

Models featuring position-dependent masses have been discussed in a wide range of areas, from semiconductors [14, 15, 16, 17] to quantum wells and quantum dots [18, 19, 20, 21], and from astrophysics [22] to polarons [23] and nonlinear optics [24]. One way to introduce the effect of dependence of the mass on the particle's position on the system's properties is to use the framework of the position-dependent effective mass Schrödinger equations [25, 26, 27]. In such cases, position dependent masses are a consequence of imperfect translational invariance, caused mainly by lattice distortions and impurities. Indeed, if they are taken into account in a adequate way, their net effect can be included in the particles mass. Such an approach, which we follow in this work, has the advantage of allowing to formally derive the corresponding tight-binding Hamiltonian, which is used as starting point for all following calculations. Once this Hamiltonian formalism is of widespread use for the investigation of many quantum systems, the derivation we present in the sequence may serve as a starting point for further studies. We emphasize that Ref. [27] presents an very amazing explanation on how the Morse potential, which has a widespread use in condensed matter physics, can be mathematically derived from the assumption of the position dependent mass.

Following Ref. [25], we start with the Schrödinger equation for a field-free particle in continuous space

$$\hat{H} = -\frac{\hbar^2}{2m}\hat{D}_\gamma^2\psi(x), \quad (1)$$

in which

$$\hat{D}_\gamma = (1 + \gamma x)\frac{d}{dx} \quad (2)$$

shall be regarded as a deformed derivative translation operator, where $\gamma \geq 0$ is a parameter associated with the position-dependent effective mass m_e of the particle.

The explicit relationship between m_e and γ is derived by using Eq. (1) to evaluate the system's average energy as

$$\begin{aligned} E = \langle H \rangle &= -\frac{\hbar^2}{8} \int dx \left\{ \frac{d}{dx} \left[\frac{d}{dx} \left(\frac{1}{m_e} \right) \right] \phi \frac{d\psi}{dx} \right. \\ &\quad \left. + \frac{2}{m_e} \phi \frac{d^2\psi}{dx^2} + \frac{d}{dx} \left[\frac{d}{dx} \left(\frac{1}{m_e} \right) \right] \phi^* \frac{d\psi^*}{dx} \right\} \end{aligned}$$

$$\left. + \frac{2}{m_e} \phi^* \frac{d^2 \psi^*}{dx^2} \right\} . \quad (3)$$

The expression $m_e \equiv m/(1 + \gamma x)^2$ is obtained by identification of the terms such that, if $\gamma \equiv 0$, the energy reduces to the usual expression for a particle with constant mass. Under the same condition, the conjugate field of ψ , expressed by $\phi = \frac{\psi^*}{(1 + \gamma x)}$ [29, 30], reduces to its usual form.

3. The equivalent tight-binding Hamiltonian

In order to move from the continuous formulation in Eqs. (1-3) to a discrete one-dimensional space, we consider that x takes N integer values x_i , where N is the number of allowed sites in a lattice. This is a crucial step in this work. Indeed, it represents an extension from the local position dependent mass, usually limited to vary within a unit cell or within a fixed width potential, to a general system with translational invariance. Nevertheless, the results we obtain in the further development depend on the product γN , much as observed for the fixed width infinite potential [25]. From the physical point of view, the mass dependency on position may then be thought as arising from a global distortion of the lattice, as a external field or continuously varying inertial effect in an optical assembled device [11].

Here, it is convenient to look for the eigenstates in terms of the basis $\psi_i(x_j) = \delta_{i,j}$ and $\phi_i(x_j) = \delta_{i,j}/(1 + \gamma x_j)$, where $\delta_{i,j}$ is the Kronecker delta. Expressing the spatial derivatives in terms of differences between the pertinent functions in two neighboring sites, the following matrix representation of the system Hamiltonian is obtained

$$\begin{aligned} H_{i,j} = & - \frac{\hbar^2}{2ma^2} \{ (1 + \gamma x_{j+1}) \delta_{i,j+1} + (1 + \gamma x_{j-1}) \delta_{i,j-1} \\ & - 2(1 + \gamma x_j) \delta_{i,j} + \frac{\gamma a}{2} [\delta_{i,j-1} - \delta_{i,j+1}] \} . \end{aligned} \quad (4)$$

Here, a is the discrete natural length associated with the lattice spacing. We define $t \equiv \hbar^2/(2ma^2)$ so that, from now on, all lengths and energies are measured, respectively, in units of a and t . We set $a = 1$ and let the coordinates along the x axis direction take the values $x_j = j$, with $j = 1, 2, 3, \dots, N$, in such a way that $\gamma x \geq 0$. Further, by setting $t = 1$ and representing the annihilation and creation fermionic operations by \hat{c}_j and \hat{c}_j^\dagger , we can write the nearest neighbor tight-binding Hamiltonian as

$$\hat{H} = \hat{H}_0 + \hat{H}_1 , \quad (5)$$

where

$$\hat{H}_0 = - \sum_j (\hat{c}_j^\dagger \hat{c}_{j+1} + \hat{c}_{j+1}^\dagger \hat{c}_j) , \quad (6)$$

and

$$\hat{H}_1 = \gamma \sum_j \left\{ 2j \hat{c}_j^\dagger \hat{c}_j + \frac{(2j+1)}{2} (\hat{c}_j^\dagger \hat{c}_{j+1} + \hat{c}_{j+1}^\dagger \hat{c}_j) \right\} . \quad (7)$$

The energy spectrum and the wave functions of the Hamiltonian (5) are obtained through $\hat{H}|\psi\rangle = E|\psi\rangle$, where the eigenstates of \hat{H} corresponding to eigenvalues E can be expanded as $|\psi\rangle = \sum_j b_j |j\rangle = \sum_j b_j \hat{c}_j^\dagger |\emptyset\rangle$, with $|\emptyset\rangle$ denoting the vacuum state. From Eqs. (5), (6) and (7), we obtain the following recurrence equation for the coefficients b_j

$$\begin{aligned} & \left(\gamma(j + \frac{1}{2}) + 1\right) b_{j+1} + \left(\gamma(j - \frac{1}{2}) + 1\right) b_{j-1} \\ & = (2\gamma j - E) b_j, \end{aligned} \quad (8)$$

which must satisfy the boundary conditions $b_0 = b_{N+1} = 0$. We would like to call the attention that the dependency of the hopping terms on the position j appears in a similar equation derived to describe the behavior of periodically driven systems [33, 34].

We observe that the problem of characterizing the spectra of \hat{H}_0 and \hat{H}_1 can be carried out exactly for each one of the operators. However, as they do not commute, the overall Hamiltonian \hat{H} could not be solved in the same way. Hence, before addressing the general problem, let us briefly take care of the eigenstates of \hat{H}_0 and \hat{H}_1 .

4. Analytical results for limiting conditions

\hat{H}_0 is the usual tight binding Hamiltonian for the homogeneous one-dimensional lattice. When $\gamma = 0$, Eq. (8) reduces to $(b_{j+1}^{(0)} + b_{j-1}^{(0)}) = -E_0 b_j^{(0)}$, which coincides with the recurrence relations of the U_j Chebyshev polynomials of the second kind of degree j . That leads to the eigenvalues $E_0(j) = -2 \cos(\frac{j\pi}{N+1})$ and wave function coefficients $b_j^{(0)} = \frac{1}{\sqrt{N+1}} \sin(\frac{j\pi}{N+1})$. This well known result characterizes Bloch extended states for all energies in the spectrum, with density of states (DOS)

$$\rho_0(E) = \frac{1}{\pi\sqrt{4 - E^2}}, \quad E \in [-2, 2] \quad (9)$$

in the $N \rightarrow \infty$ limit.

As for the eigenvalues and eigenvectors of \hat{H}_1 , we consider only the terms that are multiplied by γ in Eq. (7), which leads to

$$\left(j + \frac{1}{2}\right) b_{j+1}^{(1)} + \left(j - \frac{1}{2}\right) b_{j-1}^{(1)} = 2(j - \epsilon) b_j^{(1)}, \quad (10)$$

where ϵ indicates the scaled energy, i.e., $\epsilon = \frac{E}{\gamma}$. In the $N \gg 1$ limit and for sufficiently large j , Eq. (10) can be approximated by $(j+1)b_{j+1}^{(1)} + (j-1)b_{j-1}^{(1)} \cong 2(j - \epsilon) b_j^{(1)}$, which is the recurrence relation of the Laguerre polynomials $L_j^{(-1)}$. Using the same boundary conditions as above and taking into account the proper asymptotic expansions [31], we can write the eigenvalues as

$$E_1(j) = 4\gamma(N+1) \cos^2(\theta_j), \quad (11)$$

where $\theta_j \in (0, \pi/2)$ is obtained by the N equations

$$(N+1)[\sin(2\theta_j) - 2\theta_j] + \frac{3\pi}{4} = j\pi, \quad j = 1, 2, \dots, N. \quad (12)$$

After straightforward calculations, it is possible to show that the DOS in the $N \rightarrow \infty$ limit is given by

$$\rho_1(E) = \frac{\sqrt{E(4\gamma N - E)}}{2\gamma\pi N E} \quad E/\gamma N \in [0, 4]. \quad (13)$$

Therefore, the eigenstates of \hat{H}_1 , characterized by Laguerre polynomial coefficients, feature localized-like behavior over the whole energy spectrum. As a matter of fact, the asymptotic behavior $b_j^{(1)} \sim j^{-3/4}$ [31] shows that the wave functions decay polynomially. In seemingly contrast with the spectrum of extend states, Eq. (13) indicates that the allowed energy interval increases linearly with the size of the system for fixed γ . However, to analyze the results in the limit of large systems it is more convenient to assume the explicit dependency $\gamma N = \text{constant}$.

Fig. 1(a) shows the DOS for \hat{H}_0 and \hat{H}_1 given by, respectively, Eqs. (9) and (13). We also draw the energy density of states obtained by numerical diagonalization of the two corresponding system of $N = 8000$ sites. It is clearly shown that the approximate expression for the \hat{H}_1 (Eq. (13)) agrees with the numerical results, in such a way that, in this limit, the approximate and numerical results coalesce with the exact result for $\rho_1(E)$.

The individual solutions for \hat{H}_0 and \hat{H}_1 allows the identification of two γ dependent limiting conditions for \hat{H} . When \hat{H}_0 plays the relevant role, every energy level corresponds to a Bloch extended wave function. On the other hand, when \hat{H}_1 becomes relevant, every energy level has a Laguerre localized wave function. Therefore, the extended/localized regimes are controlled by the space dependent effective mass through the parameter γ .

5. Results for the coexistence regime

Differently from the cases when \hat{H}_0 and \hat{H}_1 control the system separately, we cannot find a general analytical solution for \hat{H} . While exact solutions in the particular limits reproduce the results for \hat{H}_0 and \hat{H}_1 , the general case requires analytical approximation approaches and the numerical method of cluster exact diagonalization. Fig. 1(b) illustrates the behavior of $\rho(E)$ for selected choices of γ in \hat{H} obtained numerically for a $N = 8000$ sites system. The numerical results consistently indicate that the energy band extends itself from $E = E_{min} = -2t$ to $E = E_{max} = 2t + 4\gamma N$, values that correspond to the sum of lower and upper bounds from the two individual models shown in Fig. 1(a). For any finite γN , the energy band is finite. In accordance to the above relation, when $\gamma = 1/N^2$ the result for $\rho_0(E)$ is recovered. More generally, our numerical investigations based on a general relation $\gamma \sim N^{-\alpha}$ suggest that, in the $N \rightarrow \infty$ limit, the upper bound converges to $2t$ if $\alpha > 1$, whereas it diverges when $\alpha < 1$. Thus, the analytical results obtained from the analysis of Eq. (10) prevails for the full Hamiltonian \hat{H} .

Three different regimes can be devised for the model:

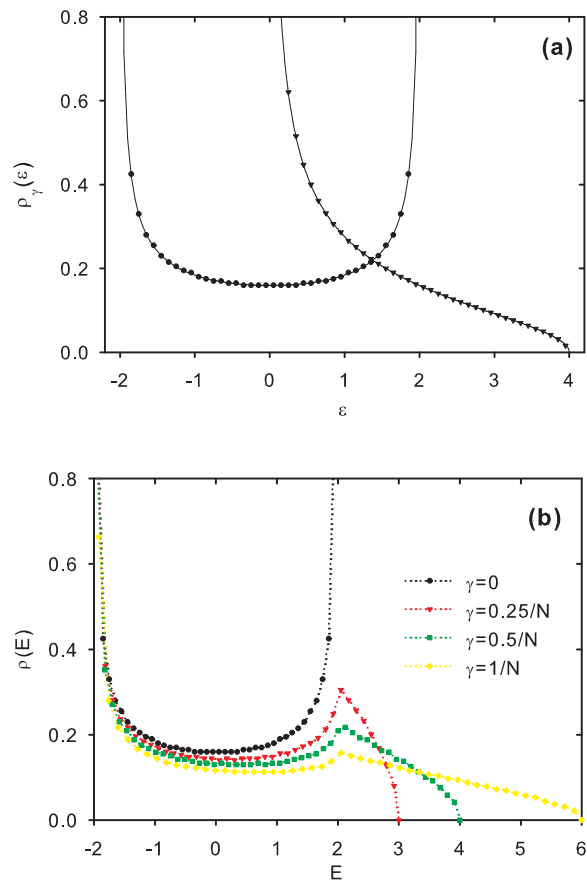


Figure 1. (a) DOS $\rho(E)$ as a function of E for \hat{H}_0 (circles) and \hat{H}_1 (triangles) for $\gamma = 1/N$ from a system of $N = 8000$ sites. Solid lines correspond to the analytical expressions in Eqs. (9) and (13). (b) DOS for \hat{H} as a function of E for some typical values of γ in the *intermediate regime*.

- (i) Bloch regime: $0 \leq \gamma < O(N^{-1})$
- (ii) Intermediate regime: $\gamma \sim O(N^{-1})$
- (iii) Localized regime: $\gamma > O(N^{-1})$

In the *Bloch regime*, it is easy to see that Eq. (8) reduces to the same form as for $\gamma = 0$. Thus, only \hat{H}_0 plays a relevant role and every energy level has a Bloch extended wave function. On the other hand, in the *localized regime* where only \hat{H}_1 is relevant, every energy level has a Laguerre localized wave function and the energy spectrum is not limited. Despite an intensive search in the literature, we were not able to find any investigation on an actual physical system where the range of values of γ satisfy this condition.

Let us then consider the *intermediate regime* as it does not only comprise our most important findings, but also allows for establishing a direct relationship to a real world application. In the case of Ge quantum dots, experimental measurements show that a interface potential is responsible for quantum confinement, the extension of which can

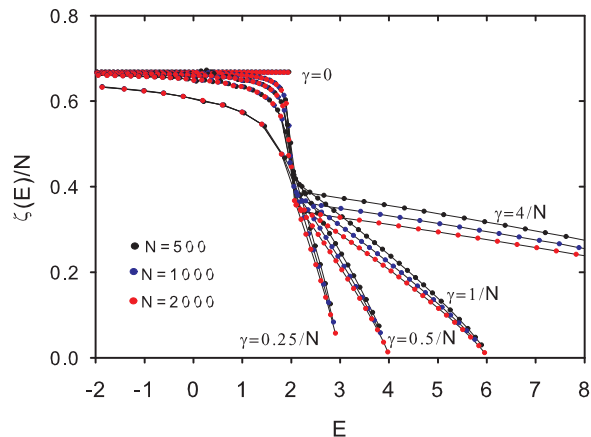


Figure 2. Dependence of $\zeta(E)$ as a function of E and N for a selected number of states in the allowed energy range. The mobility edge separating extended and localized states occurs always at $E = 2$, $\forall \gamma N$ values.

be traced back to the value of γ [20, 21]. Amazingly, within the carrier effective-mass formalism, the functional dependence between γ and the size of this region is exactly the same as that of the intermediate regime defined above.

In order to make use of analytical asymptotic expressions, let us assume the non-binding restriction $N \gg 1$. For a fixed γN , we identify the coexistence of extended and localized states. The \hat{H} eigenfunctions entail contributions from the \hat{H}_0 extended states as well as from the \hat{H}_1 localized states. However, depending on the energy eigenvalue, the eigenfunctions display more localized or extended properties. To quantify this contribution, we numerically investigated the local properties of the wave function by evaluating the participation ratio

$$\zeta(E) = \frac{1}{\sum_j |b_j(E)|^4}. \quad (14)$$

The localized or extended character of the states can be inferred from the dependency of the value of $\zeta(E)$ with respect to the system size N : it decays to zero for localized states or converges to a finite non-zero value for extended states.

Figure 2 shows the participation ratio ζ_E as a function of the energy E for $N = 500$, 1000 and 2000 and $\gamma = 0, 0.25/N, 0.5/N, 1/N$ and $4/N$. Our results show that, on increasing the value of N , ζ_E has a clear monotonic decay to 0 when $E > 2$, while it remains at a finite value when $E < 2$. Thus, the mobility edge occurs always at the value $E = 2$, irrespective of the product γN .

A further important measure to compute is the fraction of energy levels corresponding to localized and extended states and to obtain its dependency on γ . In Figure 3 we show the density of localized levels $\rho_{loc}(\gamma)$ as a function of γ in the $N \rightarrow \infty$ limit. All of such states are restricted to $E > 2$, which corresponds to the region of localized states. The results are estimated from numerical evaluations for $N = 200, 400, 800$ and 1600. The numerical results indicate that the fraction of localized levels in

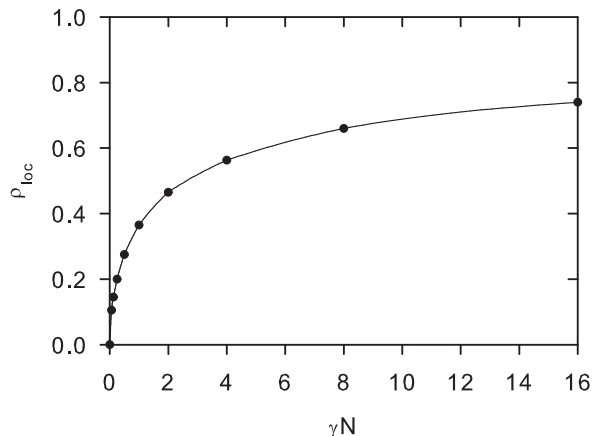


Figure 3. Behavior of $\rho_{loc}(\gamma)$ as a function of γ in the $N \rightarrow \infty$ limit. The numerical results indicate that a nonzero fraction of localized states is observed as soon as $\gamma > 0$.

the total spectrum increases with γ , but the fraction of extended states never vanishes. It is interesting to note that, in the case of free electrons in the presence of an uniform strong electric field, localized and extended states have also been found. However, the extended states are restricted to the edge of the band and the fraction of these levels in the total spectrum goes to zero at the large N limit[32].

6. Conclusions

Our results clearly indicate the coexistence of extended and localized quantum states in a simple one-dimensional system of particles with position dependent masses. Although our work goes along the same direction as recent efforts to characterize theoretical aspects of the problem [6, 10, 11, 12], its very simple form allowing for exact results does provide another point of view on the subject, which might be useful to new experimental designs [8].

The presence of a position dependent mass m_e , leading to the coupling between the momentum and position operators in the Schrödinger equation as well as in the \hat{H} Hamiltonian, is the key feature of our approach. Although the presence of linear terms in a Schrödinger equation is a common feature whenever the systems stays under the influence of electric field, the particular functional dependence caused by m_e is much richer and induced the features discussed herein. The numerical results can be traced back to well documented results that we obtained analytically for each limiting regime, in which either localized or extended states are to be found. That ultimately led us to set a well-defined energy value for the mobility edge. Besides showing the direct relationship of our results to the confinement potential in a carrier space dependent effective mass scenario, we conjecture whether the recent experimental advances indicating mobility edge transition in one-dimensional optical lattice might benefit from the robust theoretical framework reported in this work.

7. Acknowledgements

We thank G.M.A. Almeida for valuable suggestions on the manuscript and the financial support of Brazilian agency CNPq. Both authors benefit from the support of the Instituto Nacional de Ciência e Tecnologia para Sistemas Complexos (INCT-SC).

References

- [1] P. W. Anderson, Absence of Diffusion in Certain Random Lattices, *Phys. Rev.* **109**, 1492 (1958).
- [2] F. A. B. F. de Moura, and M. L. Lyra, Delocalization in the 1D Anderson Model with Long-Range Correlated Disorder, *Phys. Rev. Lett.* **81**, 3735 (1998); G. M. A. Almeida, F. A. B. F. de Moura, T. J. G. Apollaro, and M. L. Lyra, Disorder-assisted distribution of entanglement in *XY* spin chains, *Phys. Rev. A* **96**, 032315 (2017).
- [3] S. Aubry and G. Andre, Analyticity breaking and Anderson localization in incommensurate lattices, *Ann. Israel Phys. Soc.* **3**, 1 (1980).
- [4] I. Chang, Z. Lev, A. B. Harris, J. Adler, and A. Aharony, Localization Length Exponent in Quantum Percolation, *Phys. Rev. Lett.* **74**, 2094 (1995).
- [5] L. Gong and P. Tong, Localization-delocalization transitions in a two-dimensional quantum percolation model: von Neumann entropy studies, *Phys. Rev. B* **80**, 174205 (2009).
- [6] L. Jahnke, J. W. Kantelhardt, R. Berkovits, and S. Havlin, Wave Localization in Complex Networks with High Clustering, *Phys. Rev. Lett.* **101**, 175702 (2008).
- [7] O. Giraud, B. Georgeot, and D. L. Shepelyansky, Delocalization transition for the Google matrix, *Phys. Rev. E* **80**, 026107 (2009).
- [8] G. Semeghini, M. Landini, P. Castilho, S. Roy, G. Spagnolli, A. Trenkwalder, M. Fattori, M. Inguscio and G. Modugno, Measurement of the mobility edge for 3D Anderson localization, *Nat. Phys.* **11**, 554 (2015).
- [9] P. Ribeiro, M. Haque, and A. Lazarides, Strongly interacting bosons in multichromatic potentials supporting mobility edges: Localization, quasi-condensation, and expansion dynamics, *Phys. Rev. A* **87**, 043635 (2013).
- [10] M. Pasek, G. Orso, and D. Delande, Anderson Localization of Ultracold Atoms: Where is the Mobility Edge?, *Phys. Rev. Lett.* **118**, 170403 (2017).
- [11] H. P. Luschen, S. Scherg, T. Kohlert, M. Schreiber, P. Bordia, Xiao Li, S. Das Sarma, and I. Bloch, Exploring the Single-Particle Mobility Edge in a One-Dimensional Quasiperiodic Optical Lattice, *arXiv:1709.03478* (2017).
- [12] X. Li, X. Li and S. Das Sarma, Mobility edges in one-dimensional bichromatic incommensurate potentials, *Phys. Rev. B* **96**, 085119 (2017).
- [13] M. Modugno, Exponential localization in one-dimensional quasi-periodic optical lattices, *New Journal Phys.* **11**, 033023 (2009).
- [14] W. A. Harrison, Tunneling from an Independent-Particle Point of View, *Phys. Rev.* **123**, 85 (1961).
- [15] T. Gora, and F. Williams, Theory of Electronic States and Transport in Graded Mixed Semiconductors, *Phys. Rev.* **177**, 1179 (1969).
- [16] O. von Roos, Position-dependent effective masses in semiconductor theory, *Phys. Rev. B* **27**, 7547 (1983).
- [17] M. R. Geller, and W. Kohn, Quantum mechanics of electrons in crystals with graded composition, *Phys. Rev. Lett.* **70**, 3103 (1993).
- [18] P. Harrison, *Quantum Wells, Wires and Dots* (New York: Wiley, 2000).
- [19] A. Keshavarz, and N. Zamani, Optical properties of spherical quantum dot with position-dependent effective mass, *Superlatt. Microstruct.* **58**, 191 (2013).
- [20] E. G. Barbagiovanni, and R.N. Costa Filho, Quantum confinement in nonadditive space with a spatially dependent effective mass for Si and Ge quantum wells, *Physica E* **63**, 14 (2014).

- [21] E. G. Barbagiovanni, S. Cosentino, D. J. Lockwood, R. N. Costa Filho, A. Terrasi, and S. Mirabella, Influence of interface potential on the effective mass in Ge nanostructures, *Journal of Applied Physics* **117**, 154304 (2015).
- [22] D. O. Richstone and M. D. Potter, Galactic mass loss - A mild evolutionary correction to the angular size test, *Astrophys. J.* **254**, 451 (1982).
- [23] F. Q. Zhao, X. X. Liang, and S. L. Ban, Influence of the spatially dependent effective mass on bound polarons in finite parabolic quantum wells, *Eur. Phys. J. B* **33**, 3 (2003).
- [24] R. Khordad, Effect of position-dependent effective mass on linear and nonlinear optical properties in a quantum dot, *Indian J. Phys.* **86**, 513 (2012).
- [25] R. N. Costa Filho, M. P. Almeida, G. A. Farias, and J. S. Andrade Jr., Displacement operator for quantum systems with position-dependent mass, *Phys. Rev. A* **84**, 050102(R) (2011).
- [26] S. H. Mazharimousavi, Revisiting the displacement operator for quantum systems with position-dependent mass, *Phys. Rev. A* **85**, 034102 (2012).
- [27] R. N. Costa Filho, G. Alencar, B.-S. Skagerstam, and J. S. Andrade, Jr., Morse potential derived from first principles, *Europhys. Lett.* **101**, 10009 (2013).
- [28] B. G. da Costa and E. P. Borges, Generalized space and linear momentum operators in quantum mechanics, *J. Math. Phys.* **55**, 062105 (2014).
- [29] M. A. Rego-Monteiro and F. D. Nobre, Classical field theory for a non-Hermitian Schrodinger equation with position-dependent masses, *Phys. Rev. A* **88**, 032105 (2013).
- [30] M. A. Rego-Monteiro, L. M. C. S. Rodrigues, and E. M. F. Curado, Position-dependent mass quantum Hamiltonians: general approach and duality, *J. Phys. A: Math. Theor.* **49** 125203 (2016).
- [31] G. Szego. *Orthogonal polynomials* (American Mathematical Society, Rhode Island, 1975), 4nd ed.
- [32] H. Fukuyama, R. A. Bari, and H. C. Fogedby, Tightly bound electrons in a uniform electric field, *Phys. Rev. B* **8**, 5579 (1973).
- [33] R. V. Jensen, S. M. Susskind, and M. M. Sanders, Microwave ionization of highly excited hydrogen atoms: a test of the correspondence principle, *Phys. Rev. Lett.* **62**, 1476 (1989)
- [34] C.R. de Oliveira, I. Guarneri, G. Casati, From power-Localized to extended quasi-energy eigenstates in a quantum periodically driven system, *Eur. Phys. Lett.* **27**, 187 (1994).